



## LJMU Research Online

Wu, Y, Ma, X, Yu, L, Feng, X, Zhao, S, Zhang, W, Zhang, J and Hao, Y

**High-Temperature Characterization of AlGaN Channel High Electron Mobility Transistor Based on Silicon Substrate.**

<http://researchonline.ljmu.ac.uk/id/eprint/25189/>

### Article

**Citation** (please note it is advisable to refer to the publisher's version if you intend to cite from this work)

**Wu, Y, Ma, X, Yu, L, Feng, X, Zhao, S, Zhang, W, Zhang, J and Hao, Y (2024) High-Temperature Characterization of AlGaN Channel High Electron Mobility Transistor Based on Silicon Substrate. *Micromachines*, 15 (11). pp. 1-8. ISSN 2072-666X**

LJMU has developed [LJMU Research Online](#) for users to access the research output of the University more effectively. Copyright © and Moral Rights for the papers on this site are retained by the individual authors and/or other copyright owners. Users may download and/or print one copy of any article(s) in LJMU Research Online to facilitate their private study or for non-commercial research. You may not engage in further distribution of the material or use it for any profit-making activities or any commercial gain.


The version presented here may differ from the published version or from the version of the record. Please see the repository URL above for details on accessing the published version and note that access may require a subscription.

For more information please contact [researchonline@ljmu.ac.uk](mailto:researchonline@ljmu.ac.uk)

<http://researchonline.ljmu.ac.uk/>

## Article

# High-Temperature Characterization of AlGa<sub>N</sub> Channel High Electron Mobility Transistor Based on Silicon Substrate

Yinhe Wu<sup>1</sup>, Xingchi Ma<sup>1</sup>, Longyang Yu<sup>2,\*</sup>, Xin Feng<sup>1</sup> , Shenglei Zhao<sup>2</sup>, Weihang Zhang<sup>1</sup>, Jincheng Zhang<sup>2</sup> and Yue Hao<sup>2</sup>

<sup>1</sup> Guangzhou Wide Bandgap Semiconductor Innovation Center, Guangzhou Institute of Technology, Xidian University, Guangzhou 510555, China; wuyinhe@xidian.edu.cn (Y.W.); 23111213596@stu.xidian.edu.cn (X.M.); xinfeng@xidian.edu.cn (X.F.); whzhang@xidian.edu.cn (W.Z.)

<sup>2</sup> State Key Laboratory of Wide-Bandgap Semiconductor Devices and Integrated Technology, School of Microelectronics, Xidian University, Xi'an 710071, China; slzhao@xidian.edu.cn (S.Z.); jchzhang@xidian.edu.cn (J.Z.); yhao@xidian.edu.cn (Y.H.)

\* Correspondence: yulongyang@xidian.edu.cn; Tel.: +86-187-8945-1173

**Abstract:** In this paper, it is demonstrated that the AlGa<sub>N</sub> high electron mobility transistor (HEMT) based on silicon wafer exhibits excellent high-temperature performance. First, the output characteristics show that the ratio of on-resistance ( $R_{ON}$ ) only reaches 1.55 when the working temperature increases from 25 °C to 150 °C. This increase in  $R_{ON}$  is caused by a reduction in optical phonon scattering-limited mobility ( $\mu_{OP}$ ) in the AlGa<sub>N</sub> material. Moreover, the device also displays great high-performance stability in that the variation of the threshold voltage ( $\Delta V_{TH}$ ) is only 0.1 V, and the off-state leakage current ( $I_{D,off-state}$ ) is simply increased from  $2.87 \times 10^{-5}$  to  $1.85 \times 10^{-4}$  mA/mm, under the operating temperature variation from 25 °C to 200 °C. It is found that the two trap states are induced at high temperatures, and the trap state densities ( $D_T$ ) of  $4.09 \times 10^{12}$ – $5.95 \times 10^{12}$  and  $7.58 \times 10^{12}$ – $1.53 \times 10^{13}$  cm<sup>-2</sup> eV<sup>-1</sup> are located at  $E_T$  in a range of 0.46–0.48 eV and 0.57–0.61 eV, respectively, which lead to the slight performance degeneration of AlGa<sub>N</sub> HEMT. Therefore, this work provides experimental and theoretical evidence of AlGa<sub>N</sub> HEMT for high-temperature applications, pushing the development of ultra-wide gap semiconductors greatly.

**Keywords:** AlGa<sub>N</sub> channel high electron mobility transistor; high temperature; trap states; carrier mobility



**Citation:** Wu, Y.; Ma, X.; Yu, L.; Feng, X.; Zhao, S.; Zhang, W.; Zhang, J.; Hao, Y. High-Temperature Characterization of AlGa<sub>N</sub> Channel High Electron Mobility Transistor Based on Silicon Substrate.

*Micromachines* **2024**, *15*, 1343.

<https://doi.org/10.3390/mi15111343>

mi15111343

Academic Editor: Haiding Sun

Received: 29 September 2024

Revised: 25 October 2024

Accepted: 29 October 2024

Published: 31 October 2024



**Copyright:** © 2024 by the authors. Licensee MDPI, Basel, Switzerland. This article is an open access article distributed under the terms and conditions of the Creative Commons Attribution (CC BY) license (<https://creativecommons.org/licenses/by/4.0/>).

## 1. Introduction

Owing to the high electric field strength and electron mobility of the GaN material, GaN HEMTs have been widely researched and applied in power electronics [1–5]. Compared with traditional GaN materials, ultra-wide bandgap (UWBD) materials possess higher bandgaps and critical electric fields; thus, these devices based on UWBD materials have more developmental potential in power electronic applications [6–11]. Among these UWBD materials ( $\beta$ -Ga<sub>2</sub>O<sub>3</sub>, diamond, and AlN), the material growth and device fabrication of AlGa<sub>N</sub> appear to be much easier due to the relevant GaN-based heterojunction. Moreover, AlGa<sub>N</sub> HEMTs have been recognized as an excellent candidate for high-temperature applications because of their great thermal stability [12,13]. The outstanding performance of AlGa<sub>N</sub> HEMTs under extreme temperature conditions makes them an ideal choice for a wide range of applications, including aerospace, electric vehicles, radar and communication, energy conversion, and industrial automation.

For these reasons, many scholars have carried out extensive studies on the device characteristics of AlGa<sub>N</sub> HEMTs at high temperatures. Numerous valuable achievements have been obtained, including lower drain current attenuation, off-state leakage current, on-resistance degradation, channel mobility attenuation, smaller threshold voltage shift, higher breakdown electric field, saturated drain current, and current gain cut-off frequency of

AlGa<sub>N</sub> channel HEMTs compared with traditional GaN channel HEMTs [14–25]. However, most of these reports are based on sapphire and AlN substrates, and there is a lack of research on the performance and related analysis of the AlGa<sub>N</sub> HEMTs based on silicon (Si-based AlGa<sub>N</sub> HEMTs) at high temperatures. As is known, the Si-based AlGa<sub>N</sub> HEMTs have better thermal conductivity and greater commercialization potential due to the use of low-cost substrates. Therefore, it is necessary to investigate the high-temperature characteristics of Si-based AlGa<sub>N</sub> HEMTs and identify the relevant influence factors for performance degeneration so as to put forward more useful strategies to solve it.

In this work, the technology of pulsed metal–organic chemical vapor deposition (MOCVD) was used to fabricate the 6-inch AlGa<sub>N</sub> wafer on the Si substrate. Then, the Si-based AlGa<sub>N</sub> HEMT with 400 nm Al<sub>0.1</sub>Ga<sub>0.9</sub>N as a channel layer was fabricated and showed a low contact resistance of 0.95 Ω·mm and a high breakdown voltage of 1110 V (with  $L_{GD} = 15 \mu\text{m}$ ). In addition, the output and transfer characteristics of this device at high-temperature working conditions were systematically investigated. Using the alternating current conductance method, the trapping effect in the AlGa<sub>N</sub> channel was characterized by time constants ( $\tau_T$ ) and  $D_T$ , which helped to explain the performance degradation. Overall, given the cost advantages of Si-based AlGa<sub>N</sub> HEMTs, this study provides valuable references for future design optimizations of such devices and also lays the theoretical foundation for their practical applications in harsh environments, such as those involving high temperatures and high powers.

## 2. Materials and Methods

The pulsed MOCVD system was used to grow AlGa<sub>N</sub> material on a 6-inch Si substrate. Firstly, an AlN nucleation layer was deposited. Then, a 3 μm graded Al<sub>x</sub>Ga<sub>1-x</sub>N layer, 1 μm C-doped Al<sub>0.1</sub>Ga<sub>0.9</sub>N layer, 400 nm Al<sub>0.1</sub>Ga<sub>0.9</sub>N channel layer, 1 nm AlN insertion layer, 24 nm Al<sub>0.4</sub>Ga<sub>0.6</sub>N barrier layer, and 2 nm GaN cap layer were grown above the AlN nucleation layer as a sequence. The HRXRD rocking curves from (0002) and (10–12) planes of the AlGa<sub>N</sub> channel layer in this work are 708 and 1147 arcsec, respectively.

The fabrication process of AlGa<sub>N</sub> HEMTs began with mesa isolation etching. Thereafter, a 30 nm recess was etched accurately using the inductively coupled plasma (ICP) technique, and the Ti/Al alloy was deposited and annealed to form ohmic contact as a source/drain electrode. The Ni/Al alloy was deposited as a gate electrode. Finally, 40 nm Al<sub>2</sub>O<sub>3</sub> was grown on the surface of AlGa<sub>N</sub> HEMTs by plasma-enhanced atomic layer deposition (PEALD) to suppress the effect of surface states. The device tested in this work had a gate width ( $W_G$ ) of 100 μm, a gate length ( $L_G$ ) of 4 μm, a gate–source distance ( $L_{GS}$ ) of 4 μm, and a gate–drain distance ( $L_{GD}$ ) of 15 μm. The cross-sectional structure of AlGa<sub>N</sub> HEMT is shown in Figure 1. The output and transfer characteristics were tested using the Agilent B1505A high-voltage semiconductor analyzer system (Keysight Technologies, Beijing, China).

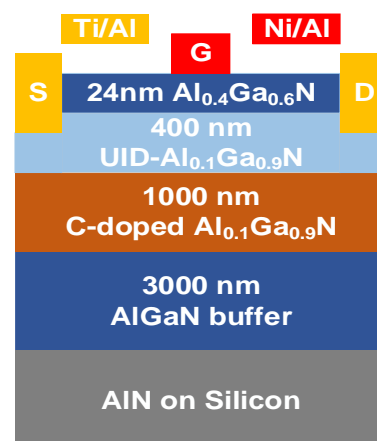


**Figure 1.** The cross-sectional structure of Si-based AlGa<sub>N</sub> HEMT.

### 3. Results and Discussion

As shown in Figure 2a, the DC output characteristics of Si-based AlGaIn HEMTs were measured at 25~200 °C with a growing step of 25 °C under a given  $V_G$  of 3 V. At 25 °C, the maximum output current ( $I_{D,max}$ ) of the AlGaIn HEMTs is 323.14 mA/mm, displaying a gradually decreasing trend as the temperature rises. The  $I_{D,max}$  still maintains values of 212.04 and 189.50 mA/mm at high temperatures of 150 and 200 °C, respectively. So, the ratio  $R_{ON,150\text{ }^\circ\text{C}}/R_{ON,25\text{ }^\circ\text{C}}$  for the Si-based AlGaIn HEMT is only 1.55 in this work, which is significantly lower than the corresponding values of commercial GaN HEMTs on silicon (the values of  $R_{ON,150\text{ }^\circ\text{C}}/R_{ON,25\text{ }^\circ\text{C}}$  of the GaN systems GS 66516B and GS 66502B are about 2.58). Therefore, the Si-based AlGaIn HEMT demonstrates more stable output characteristics compared with GaN HEMTs at high-temperature applications [9,10].

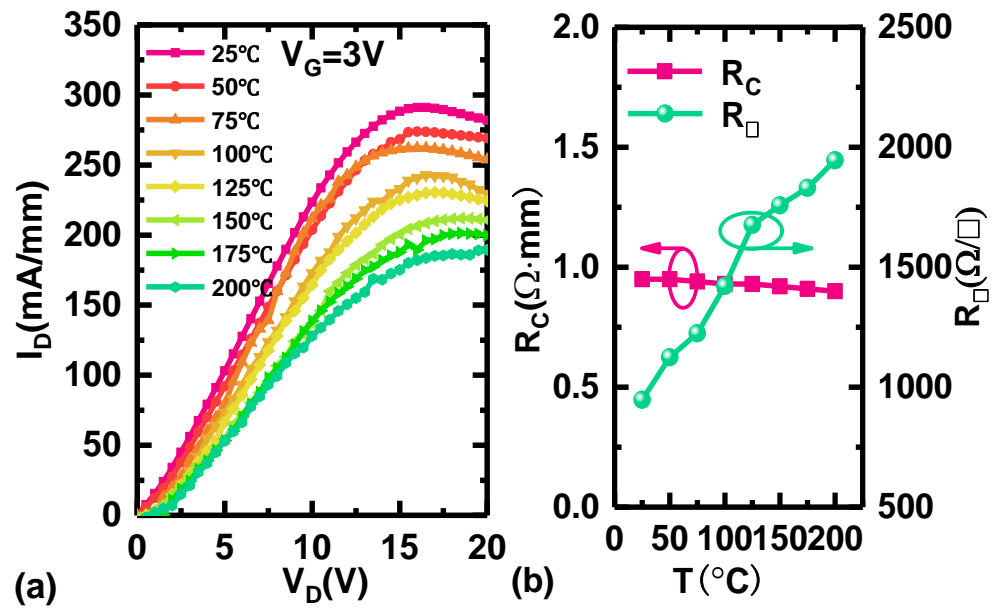


**Figure 2.** (a) The output characteristics of Si-based AlGaIn HEMT at 25/50/75/100/125/150/175/200 °C. (b) The variation of  $R_C$  and  $R_{SH}$  at different temperatures.

The degeneration of  $I_{D,max}$  at high temperatures may be caused by an increase in ohmic contact resistance ( $R_C$ ) and 2DEG channel resistance ( $R_{CH}$ ).  $R_{ON}$  can be realized as  $R_{ON} = R_S + R_D + 2R_C + R_{CH}$ .  $R_S$  or  $R_D$  is the parasitic source/drain resistance. Usually,  $R_S$  and  $R_D$  are much lower than  $R_C$ . As shown in Figure 2b,  $R_C$  is calculated using a transmission line model (TLM) at different temperatures. The variation of  $R_C$  is very poor with the growing temperature. Compared with the variation of  $R_{ON}$ , the variation of  $R_C$  is negligible. However, it is observed that the sheet resistance ( $R_{SH}$ ) increases from 947.0  $\Omega/\square$  to 1945.7  $\Omega/\square$  as the temperature rises from 25 °C to 200 °C, indicating that the rise in  $R_{ON}$  can be attributed to increased channel resistance, which can be interpreted as decreased carrier mobility.

The temperature-dependent C-V characteristics of the Schottky barrier diode with an AlGaIn channel are shown in Figure 3a. The electron concentration of the AlGaIn channel varied with the temperature-dependent depth profiles and are derived by the following Equations (1) and (2) [26,27], and the relevant results are shown in Figure 3b:

$$Z = \epsilon A / C \tag{1}$$

$$n_c = -\frac{2}{\epsilon \epsilon_0 A^2} \times \frac{1}{d(1/c^2)/dV^q} \tag{2}$$

$$n_{2DEG} = \int_{-\infty}^{+\infty} n_c(Z) dZ \tag{3}$$

$$\mu = 1/(R_{SH} \times n_s \times q) \tag{4}$$

where  $Z$  is the depth to the gate,  $\epsilon$  is the dielectric constant of the barrier,  $C$  is the junction capacitor, and  $A$  is the area of the junction capacitor. The dielectric constant used in this work is  $\epsilon_{r,Al_{0.4}Ga_{0.6}N} = 8.66$ . The  $n_{2DEG}$  is approximately calculated by Equation (3). As shown in Figure 3c, with a temperature increase, the variation of  $n_{2DEG}$  is very poor.

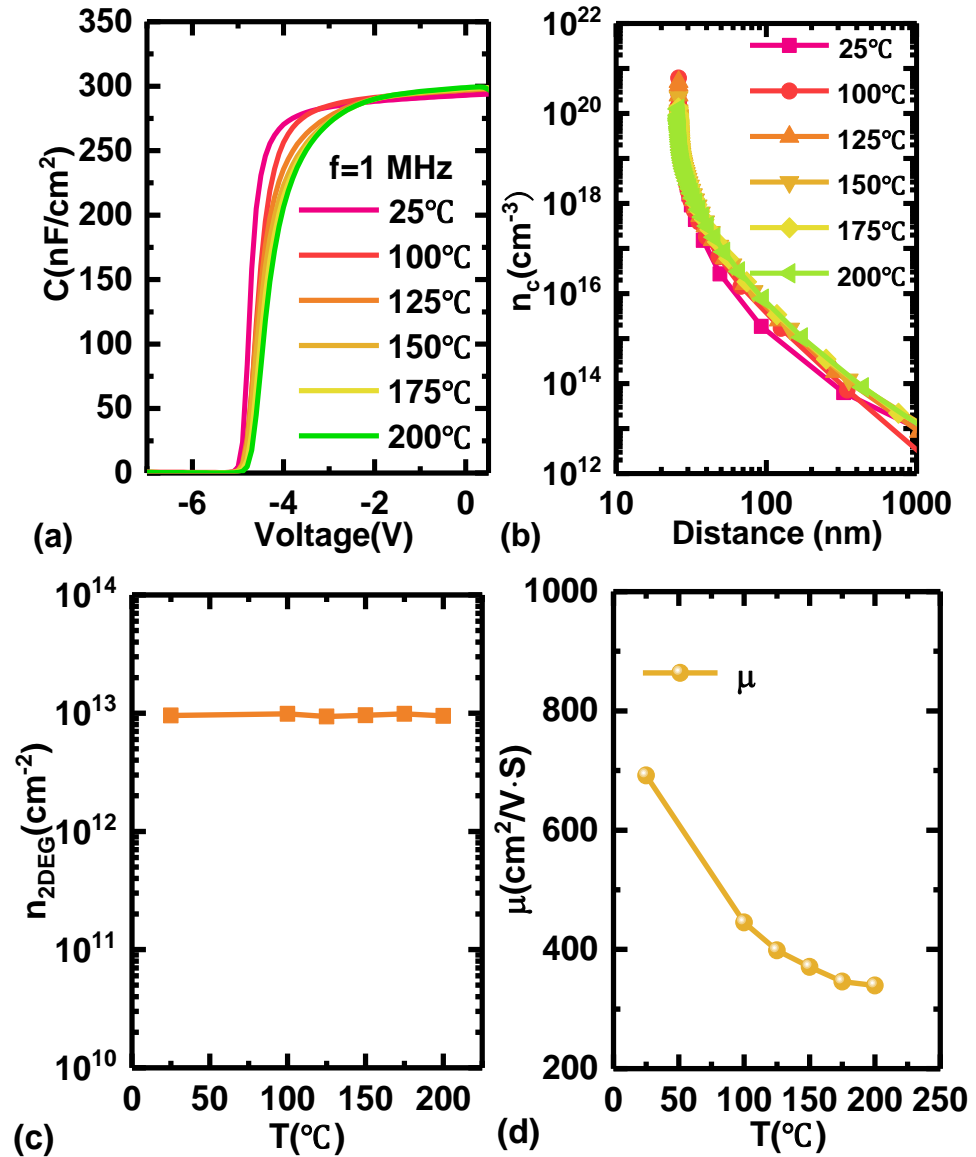


**Figure 3.** (a) The temperature-dependent C-V characteristics of the Schottky barrier diode on the AlGa<sub>N</sub> channel. (b) The value of carrier concentration with the variation of channel depth. (c) The temperature-dependent 2DEG sheet density ( $n_{2DEG}$ ). (d) The variation of carrier mobility in the AlGa<sub>N</sub> channel with the increasing temperature.

As shown in Figure 3d, the carrier mobility of the AlGa<sub>N</sub> channel ( $\mu_{AlGaN}$ ) is approximately calculated according to Equation (4) [28], which decreases from 691.58 to 339.47 cm<sup>2</sup>/V·s as the temperature increases from 25 °C to 200 °C, and it is in good agreement with the simulation result obtained by alloy scattering-limited and optical phonon-limited mobility models [13]. As is known, the  $\mu_{AlGaN}$  is affected jointly by alloy disorder scattering and optical phonon scattering, where  $\mu_{OP}$  is very sensitive to temperature and alloy scattering-limited mobility ( $\mu_{alloy}$ ) is inverse [13]. When the temperature rises, the

influence of  $\mu_{OP}$  is gradually reduced while part of  $\mu_{alloy}$  still remains stable, leading to the idea that the AlGaN HEMTs have very excellent output characteristics under high-temperature conditions, something which is lacking in the GaN HEMTs because  $\mu_{OP}$  is very dominating in terms of carrier mobility.

Furthermore, the transfer characteristics of AlGaN HEMTs were measured at 25~200 °C with a step of 25 °C under a  $V_D$  of 10 V and are shown in Figure 4a.  $V_{TH}$  shifts slightly towards a positive direction, from -4.6 V to -4.5 V, as the temperature increases.  $I_{D,off-state}$  also increases marginally from  $2.87 \times 10^{-5}$  to  $1.85 \times 10^{-4}$  mA/mm. Additionally, the buffer leakage current ( $I_{buffer}$ ) measured with an isolated active-area mesa structure is only  $9.5 \times 10^{-8}$  mA/mm at 200 °C, which is significantly lower than  $I_{D,off-state}$ . Therefore, an increase in  $I_{D,off-state}$  at high temperatures is attributed to the reverse gate leakage current, as shown in Figure 4b. And it can be suppressed by optimizing the barrier layer or adopting a metal–insulator–semiconductor (MIS) structure.

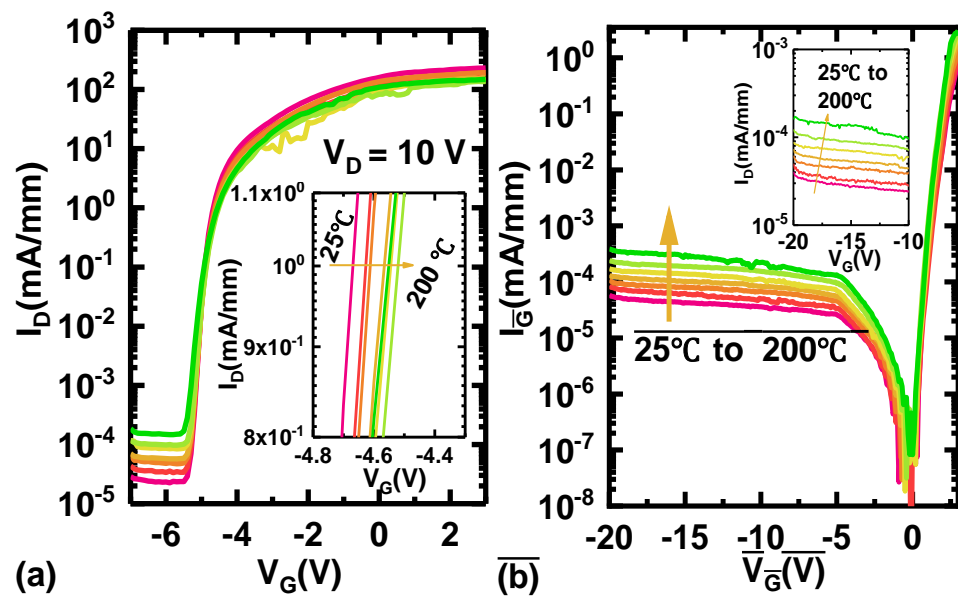


Figure 4. (a) The transfer characteristics of Si-based AlGaN HEMTs at 25/75/100/125/150/175/200 °C with an applied  $V_D$  of 10 V. (b) The forward and reverse I-V characteristics of the Schottky barrier diode in the AlGaN channel at different temperatures.

The AC capacitance technique was used to characterize the trapping effect on AlGaN HEMTs at a room temperature of 25 °C and a high temperature of 200 °C. The frequency ranged from 1 kHz to 300 kHz. As shown in Figure 5a,b, the conductance gradually increases and then decreases with the growing radial frequency. It is observed that only one conductance peak exists for a given  $V_G$  at 25 °C in Figure 5a, which can be assumed as only one kind of trap state existing in the AlGaN channel. However, there are two conductance peaks occurring at 200 °C in Figure 5b, indicating that two kinds of trap states exist in the AlGaN channel under high-temperature conditions.

Here, the plots in Figure 5a,b are effectively fitted as these curves by the following equations, respectively:

$$\frac{G_p}{\omega} = \frac{q\omega\tau_T D_T}{1 + (\omega\tau_T)^2} \tag{5}$$

$$\frac{G_p}{\omega} = \frac{q\omega\tau_{T,1} D_{T,1}}{1 + (\omega\tau_{T,1})^2} + \frac{q\omega\tau_{T,2} D_{T,2}}{1 + (\omega\tau_{T,2})^2} \tag{6}$$

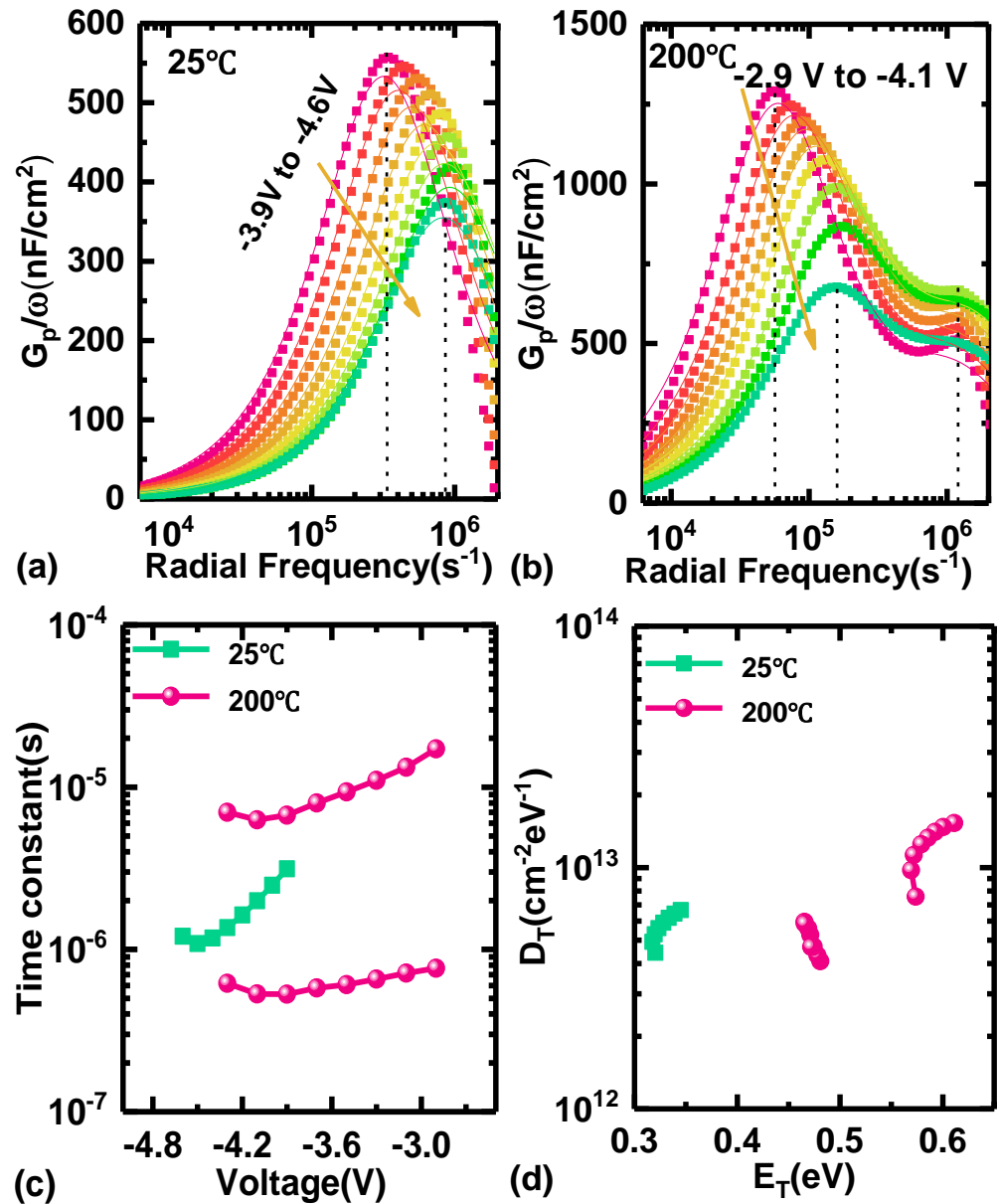


**Figure 5.** Conductance as a function of radial frequency for Si-based AlGaN HEMTs at (a) 25 °C and (b) 200 °C. (c) The time constant of trap states as a function of gate voltage. (d) The trap state density as a function of their energy.

Therefore, the time constant ( $\tau_T$ ) and trap  $D_T$  can be extracted from the above equations. The relationship between  $\tau_T$  and the applied gate voltage is depicted in Figure 5c at 25 °C and 200 °C, respectively, where  $\tau_T$  is distributed in the range of 1.08~3.13  $\mu$ s for the device working on 25 °C but two types of values of 0.53~0.77  $\mu$ s and 6.29~17.2  $\mu$ s for that on 200 °C, indicating the existence of two kinds of trap states at the same time. So, these states can be calculated by the equation as follows:

$$\tau_T = (\sigma_T N_c v_T)^{-1} \exp(E_T/kT) \tag{7}$$

Here, the cross-section of the trap states ( $\sigma_T$ ) is captured as  $3.4 \times 10^{-15} \text{ cm}^{-2}$ , and the density of states in the conduction band ( $N_c$ ) is  $2.2 \times 10^{18} \text{ cm}^{-3}$ . The average thermal velocity of carriers ( $v_T$ ) is  $2.6 \times 10^7$  and  $1.69 \times 10^7 \text{ cm/s}$  for 25 and 200 °C, respectively. As shown in Figure 5d,  $D_T$  from the range of  $4.43 \times 10^{12}$ ~ $6.67 \times 10^{12} \text{ cm}^{-2} \text{ eV}^{-1}$  is located at  $E_T$  in a range of 0.32~0.35 eV at 25 °C. But when the temperature increases to 200 °C,

$D_T$  with a distribution of  $4.09 \times 10^{12} \sim 5.95 \times 10^{12}$  and  $7.58 \times 10^{12} \sim 1.53 \times 10^{13} \text{ cm}^{-2} \text{ eV}^{-1}$  is obviously located at  $E_T$  in the range of 0.46~0.48 eV and 0.57~0.61 eV, respectively. Compared with the reported trapping effects in AlGaN materials on sapphire by Zhao's work [29], the  $\tau_T$  and  $D_T$  of trap states are much lower in the AlGaN material on silicon, indicating that the AlGaN epilayer material quality has improved significantly.

#### 4. Conclusions

In summary, the high-temperature characteristics of the Si-based AlGaN HEMTs are studied sufficiently in this work. The carrier mobility of the AlGaN channel still remains at  $339.47 \text{ cm}^2/\text{v}\cdot\text{s}$  when the working temperature reaches  $200 \text{ }^\circ\text{C}$ , and  $I_{D,\text{max}}$  still reaches up to  $189.50 \text{ mA/mm}$ . Moreover, only a positive voltage drift of  $0.1 \text{ V}$  occurs, and  $I_{D,\text{off-state}}$  increases marginally from  $2.87 \times 10^{-5}$  to  $1.85 \times 10^{-4} \text{ mA/mm}$ , strongly proving the outstanding working performance of Si-based AlGaN HEMTs compared with GaN at high temperatures. Finally, the inner trapping effect in Si-based AlGaN materials is investigated using the AC capacitance technique. Two types of trap states are found at a high temperature of  $200 \text{ }^\circ\text{C}$ . The first type of trap state has a  $D_T$  ranging from  $4.09 \times 10^{12}$  to  $5.95 \times 10^{12} \text{ cm}^{-2} \text{ eV}^{-1}$  and is located within an  $E_T$  of 0.46 to 0.48 eV. The second type of trap state has a  $D_T$  ranging from  $7.58 \times 10^{12}$  to  $1.53 \times 10^{13} \text{ cm}^{-2} \text{ eV}^{-1}$  and is located within an  $E_T$  of 0.57 to 0.61 eV. Hence, this work is very valuable for Si-based AlGaN materials as the channel for HEMTs, especially for high-temperature applications, and significantly pushes the development of ultra-wide bandgap semiconductors in power electronics.

**Author Contributions:** Conceptualization, Y.W. and L.Y.; investigation, Y.W., X.M. and L.Y.; resources, X.F., S.Z. and W.Z.; data curation, Y.W., X.M., X.F. and W.Z.; funding acquisition, Y.W. and X.F.; writing—original draft preparation, Y.W., X.F. and W.Z.; writing—review and editing, X.M., S.Z., J.Z. and Y.H.; supervision, Y.H.; project administration, L.Y., S.Z. and J.Z. All authors have read and agreed to the published version of the manuscript.

**Funding:** This research was funded by Postdoctoral Fellowship Program of CPSF (No.GZC20232055), China Postdoctoral Science Foundation (No. 2024M752521), National Natural Science Foundation of China (Grant No. 62304170 and 62374122) and Xidian University Specially Funded Project for Interdisciplinary Exploration (No. TZJH2024057).

**Data Availability Statement:** The original contributions presented in the study are included in the article, further inquiries can be directed to the corresponding author.

**Conflicts of Interest:** The authors declare no conflict of interest.

#### References

1. Xiao, M.; Du, Z.; Xie, J.; Beam, E.; Yan, X.; Cheng, K.; Wang, H.; Cao, Y.; Zhang, Y. Lateral p-GaN/2DEG junction diodes by selective-area p-GaN trench-filling-regrowth in AlGaN/GaN. *Appl. Phys. Lett.* **2020**, *116*, 053503. [\[CrossRef\]](#)
2. Lyu, Q.; Jiang, H.; Lau, K.M. High gain and high ultraviolet/visible rejection ratio photodetectors using p-GaN/AlGaN/GaN heterostructures grown on Si. *Appl. Phys. Lett.* **2020**, *117*, 071101. [\[CrossRef\]](#)
3. Ruzzarin, M.; De Santi, C.; Yu, F.; Fatahilah, M.F.; Stempel, K.; Wasisto, H.S.; Waag, A.; Meneghesso, G.; Zanoni, E.; Meneghini, M. Highly stable threshold voltage in GaN nanowire FETs: The advantages of p-GaN channel/Al<sub>2</sub>O<sub>3</sub> gate insulator. *Appl. Phys. Lett.* **2020**, *117*, 203501. [\[CrossRef\]](#)
4. Li, B.; Yang, X.; Wang, K.; Zhu, H.; Wang, L.; Chen, W. A Compact Double-Sided Cooling 650V/30A GaN Power Module With Low Parasitic Parameters. *IEEE Trans. Power Electron.* **2022**, *37*, 426–439. [\[CrossRef\]](#)
5. Murray, S.K.; Kachura, A.; Trescases, O. A 400 V Dual-Phase Series-Capacitor Buck Converter GaN IC with Integrated Closed-Loop Control. *IEEE Trans. Power Electron.* **2024**, *39*, 9579–9590. [\[CrossRef\]](#)
6. Goto, K.; Nakahata, H.; Murakami, H.; Kumagai, Y. Temperature dependence of Ga<sub>2</sub>O<sub>3</sub> growth by halide vapor phase epitaxy on sapphire and  $\beta$ -Ga<sub>2</sub>O<sub>3</sub> substrates. *Appl. Phys. Lett.* **2020**, *117*, 222101. [\[CrossRef\]](#)
7. Ren, Z.; Lv, D.; Xu, J.; Zhang, J.; Zhang, J.; Su, K.; Zhang, C.; Hao, Y. High temperature (300 °C) ALD grown Al<sub>2</sub>O<sub>3</sub> on hydrogen terminated diamond: Band offset and electrical properties of the MOSFETs. *Appl. Phys. Lett.* **2020**, *116*, 013503. [\[CrossRef\]](#)
8. Cho, Y.; Encomendero, J.; Ho, S.-T.; Xing, H.G.; Jena, D. N-polar GaN/AlN resonant tunneling diodes. *Appl. Phys. Lett.* **2020**, *117*, 143501. [\[CrossRef\]](#)



9. Visalli, D.; Van Hove, M.; Derluyn, J.; Degroote, S.; Leys, M.; Cheng, K.; Germain, M.; Borghs, G. AlGaN/GaN/AlGaN Double Heterostructures on Silicon Substrates for High Breakdown Voltage Field-Effect Transistors with low On-Resistance. *Jpn. J. Appl. Phys.* **2009**, *48*, 04C101. [[CrossRef](#)]
10. Freedman, J.J.; Hamada, T.; Miyoshi, M.; Egawa, T. Al<sub>2</sub>O<sub>3</sub>/AlGaN Channel Normally-Off MOSFET on Silicon With High Breakdown Voltage. *IEEE Electron. Device Lett.* **2017**, *38*, 497–500. [[CrossRef](#)]
11. Singhal, J.; Chaudhuri, R.; Hickman, A.; Protasenko, V.; Xing, H.G.; Jena, D. Toward AlGaN channel HEMTs on AlN: Polarization-induced 2DEGs in AlN/AlGaN/AlN heterostructures. *APL Mater.* **2022**, *10*, 111120. [[CrossRef](#)]
12. Ji, D.; Ercan, B.; Benson, G.; Newaz, A.K.M.; Chowdhury, S. 60 A/W high voltage GaN avalanche photodiode demonstrating robust avalanche and high gain up to 525 K. *Appl. Phys. Lett.* **2020**, *116*, 211102. [[CrossRef](#)]
13. Bajaj, S.; Hung, T.-H.; Akyol, F.; Nath, D.; Rajan, S. Modeling of high composition AlGaN channel high electron mobility transistors with large threshold voltage. *Appl. Phys. Lett.* **2014**, *105*, 263503. [[CrossRef](#)]
14. Carey, P.H.; Ren, F.; Baca, A.G.; Klein, B.A.; Allerman, A.A.; Armstrong, A.M.; Douglas, E.A.; Kaplar, R.J.; Kotula, P.G.; Pearton, S.J. Extreme Temperature Operation of Ultra-Wide Bandgap AlGaN High Electron Mobility Transistors. *IEEE Trans. Semicond. Manuf.* **2019**, *32*, 473–477. [[CrossRef](#)]
15. Carey, P.H.; Ren, F.; Baca, A.G.; Klein, B.A.; Allerman, A.A.; Armstrong, A.M.; Douglas, E.A.; Kaplar, R.J.; Kotula, P.G.; Pearton, S.J. Operation Up to 500 °C of Al<sub>0.85</sub>Ga<sub>0.15</sub>N/Al<sub>0.7</sub>Ga<sub>0.3</sub>N High Electron Mobility Transistors. *IEEE J. Electron. Devices Soc.* **2019**, *7*, 444–452. [[CrossRef](#)]
16. Baca, A.G.; Armstrong, A.M.; Allerman, A.A.; Klein, B.A.; Douglas, E.A.; Sanchez, C.A.; Fortune, T.R. High Temperature Operation of Al<sub>0.45</sub>Ga<sub>0.55</sub>N/Al<sub>0.30</sub>Ga<sub>0.70</sub>N High Electron Mobility Transistors. *ECS J. Solid. State Sci. Technol.* **2017**, *6*, S3010–S3013. [[CrossRef](#)]
17. Bassaler, J.; Mehta, J.; Abid, I.; Konczewicz, L.; Juillaguet, S.; Contreras, S.; Rennesson, S.; Tamariz, S.; Nemoz, M.; Semond, F.; et al. Al-Rich AlGaN Channel High Electron Mobility Transistors on Silicon: A Relevant Approach for High Temperature Stability of Electron Mobility. *Adv. Electron. Mater.* **2024**, 2400069. [[CrossRef](#)]
18. Chatterjee, B.; Lundh, J.S.; Song, Y.; Shoemaker, D.; Baca, A.G.; Kaplar, R.J.; Beechem, T.E.; Saltonstall, C.; Allerman, A.A.; Armstrong, A.M.; et al. Interdependence of Electronic and Thermal Transport in Al<sub>x</sub>Ga<sub>1-x</sub>N Channel HEMTs. *IEEE Electron. Device Lett.* **2020**, *41*, 461–464. [[CrossRef](#)]
19. Hatano, M.; Yafune, N.; Tokuda, H.; Yamamoto, Y.; Hashimoto, S.; Akita, K.; Kuzuhara, M. Superior DC and RF Performance of AlGaN-Channel HEMT at High Temperatures. *IEICE Trans. Electron.* **2012**, *E95.C*, 1332–1336. [[CrossRef](#)]
20. Li, L.; Yamaguchi, R.; Wakejima, A. Polarization engineering via InAlN/AlGaN heterostructures for demonstration of normally-off AlGaN channel field effect transistors. *Appl. Phys. Lett.* **2020**, *117*, 152108. [[CrossRef](#)]
21. Li, X.; Zhang, W.; Fu, M.; Zhang, J.; Jiang, H.; Guo, Z.; Zou, Y.; Jiang, R.; Shi, Z.; Hao, Y. AlGaN channel MIS-HEMTs with a very high breakdown electric field and excellent high-temperature performance. *IEICE Electron. Express* **2015**, *12*, 20150694. [[CrossRef](#)]
22. Mollah, S.; Gaevski, M.; Hussain, K.; Mamun, A.; Chandrashekar, M.; Simin, G.; Khan, A. Temperature characteristics of high-current UWBG enhancement and depletion mode AlGaN-channel MOSHFETs. *Appl. Phys. Lett.* **2020**, *117*, 232105. [[CrossRef](#)]
23. Tokuda, H.; Hatano, M.; Yafune, N.; Hashimoto, S.; Akita, K.; Yamamoto, Y.; Kuzuhara, M. High Al Composition AlGaN-Channel High-Electron-Mobility Transistor on AlN Substrate. *Appl. Phys. Express* **2010**, *3*, 121003. [[CrossRef](#)]
24. Zhang, L.; Zhang, J.-F.; Zhang, W.-H.; Zhang, T.; Xu, L.; Zhang, J.-C.; Hao, Y. Robust Performance of AlGaN-Channel Metal-Insulator-Semiconductor High-Electron-Mobility Transistors at High Temperatures. *Chin. Phys. Lett.* **2017**, *34*, 128501. [[CrossRef](#)]
25. Zhang, W.; Zhang, J.; Xiao, M.; Zhang, L.; Hao, Y. High Breakdown-Voltage (>2200 V) AlGaN-Channel HEMTs With Ohmic/Schottky Hybrid Drains. *IEEE J. Electron. Devices Soc.* **2018**, *6*, 931–935. [[CrossRef](#)]
26. Arulkumar, S.; Egawa, T.; Ishikawa, H.; Jimbo, T. High-temperature effects of AlGaN/GaN high-electron-mobility transistors on sapphire and semi-insulating SiC substrates. *Appl. Phys. Lett.* **2002**, *80*, 2186–2188. [[CrossRef](#)]
27. Krispin, P.; Spruytte, S.G.; Harris, J.S.; Ploog, K.H. Electrical depth profile of p-type GaAs/Ga(As, N)/GaAs heterostructures determined by capacitance–voltage measurements. *J. Appl. Phys.* **2000**, *88*, 4153–4158. [[CrossRef](#)]
28. Baca, A.G.; Armstrong, A.M.; Douglas, E.A.; Sanchez, C.A.; King, M.P.; Coltrin, M.E.; Fortune, T.R.; Kaplar, R.J. An AlN/Al<sub>0.85</sub>Ga<sub>0.15</sub>N high electron mobility transistor. *Appl. Phys. Lett.* **2016**, *109*, 033509. [[CrossRef](#)]
29. Zhao, S.; Zhang, K.; Ha, W.; Chen, Y.; Zhang, P.; Zhang, J.; Ma, X.; Hao, Y. Trap states in AlGaN channel high-electron-mobility transistors. *Appl. Phys. Lett.* **2013**, *103*, 212106. [[CrossRef](#)]

**Disclaimer/Publisher’s Note:** The statements, opinions and data contained in all publications are solely those of the individual author(s) and contributor(s) and not of MDPI and/or the editor(s). MDPI and/or the editor(s) disclaim responsibility for any injury to people or property resulting from any ideas, methods, instructions or products referred to in the content.